

Received July 5, 2019, accepted July 15, 2019, date of publication July 18, 2019, date of current version August 9, 2019.

Digital Object Identifier 10.1109/ACCESS.2019.2929868

Effect of 3D Unidirectional and Hybrid SAGE on Electromagnetic Torque Fluctuation Characteristics in Synchronous Generator

YU-LING HE¹, (Member, IEEE), MING-XING XU¹, JING XIONG², YUE-XIN SUN¹,
XIAO-LONG WANG¹, DAVID GERADA³, AND GAURANG VAKIL³, (Member, IEEE)

¹Department of Mechanical Engineering, North China Electric Power University, Baoding 071003, China

²Department of Electrical Engineering, North China Electric Power University, Baoding 071003, China

³Department of Electrical and Electronics Engineering, University of Nottingham, Nottingham NG7 2RD, U.K.

Corresponding author: Xiao-Long Wang (wangxiaolong0312@126.com)

This work was supported in part by the National Natural Science Foundation of China under Grant 51777074, in part by the Chinese Fundamental Research Funds for the Central Universities under Grant 2018YQ03, and in part by the Hebei Provincial Top Youth Talent Support Program under Grant [2018]-27.

ABSTRACT This paper presents a comprehensive study on the variation laws of electromagnetic torque (EMT) under static air-gap eccentricity (SAGE) conditions in synchronous generators. Different from other studies, this paper focuses on not only the impact of radial SAGE, but also the effect of axial and hybrid SAGE, on the EMT fluctuation characteristics, i.e., we actually study the 3D static rotor eccentricity. The theoretical analysis model is first set up to study the influence of SAGE on the magnetomotive force (MFD) and EMT. Then, the finite element calculation and the experimental study on the CS-5 prototype generator which is of two poles and 3000 rpm are carried out to validate the theoretical analysis. It is shown that the radial SAGE will increase the dc component of MFD and shift the whole MFD curve and the phase current upwardly, while the axial SAGE will reduce the dc component as well as the amplitudes of both the MFD and the phase current like a compressing operation. In general, no matter in unidirectional or hybrid SAGE cases, the radial SAGE will intensify the EMT ripple and increase each harmonic of EMT, while axial SAGE will play the opposite role. The research conclusion obtained in this paper is potential to be applied as a supplement criterion for the condition monitoring and control of the eccentricity faults.

INDEX TERMS Synchronous generator, 3D rotor eccentricity, electromagnetic torque.

ABBREVIATION

SAGE	Static air-gap eccentricity
RSAGE	Radial static air-gap eccentricity
ASAGE	Axial static air-gap eccentricity
HSAGE	Hybrid static air-gap eccentricity
EMT	Electromagnetic torque
EMF	Electromotive force
MMF	Magnetomotive force
PPUA	Permeance per unit area
MFD	Magnetic flux density

NOMENCLATURE

g_0, g	normal and RSAGE radial air-gap length
μ_0	permeability of the air
Λ_0, Λ	Constant and variable PPUA
δ_s	relative SAGE in radial direction
z	relative SAGE in axial direction
ω, ω_r	electrical and mechanical angular frequency
t	time
α_m	mechanical circumferential angle
I	Stator phase current
E_0	Exciting EMF of generator
F_r, F_s	rotor and stator MMFs in normal condition
F_{r1}, F_{s1}	rotor and stator MMFs in axial SAGE cases

The associate editor coordinating the review of this manuscript and approving it for publication was Gongbo Zhou.

F_C, F_{C1}	composite MMF before and after axial SAGE
β, β_1	angle between composite and rotor MMFs
Ψ	internal power angle of generator
φ	power factor angle
T_e	EMT
L	Effective winding length in normal condition
R, R_0	Rotor radius and inner radius of stator core
p	number of pole-pairs
P	power of generator
W	air-gap magnetic energy
U_a, U_b, U_c	three phase voltages
I_a, I_b, I_c	three phase currents
I_f	exciting current of generator

I. INTRODUCTION

Since it is very hard to keep the rotor center in strict accord with respect to the stator center, the static air-gap eccentricity (SAGE) which is also called static rotor eccentricity by many scholars [1], [2], exists in almost every motor/generator due to many factors [3]. It can be caused by un-proper assembly, bearing damage, deformation of stator core, etc., [4]–[6]. SAGE will not only bring in magnetic field distortion, but also intensify the stator and rotor vibrations [6], [7] and aggravate the wearing of the winding insulation.

Scholars have paid much attention to the magnetic field and the unbalanced magnetic pull (UMP) analysis in SAGE cases. The definition and the rotor vibration under SAGE in turbo-generator were early presented by Rosenberg in 1955 [8]. It is shown that SAGE will produce a double fundamental frequency ripples in the rotor current of salient-pole synchronous machines [9]. It will also stimulate additional currents to circulate in the stator and turn into $2(p \pm 1)$ -pole rotating space vectors in the complex domain [10], [11]. What's more, SAGE will generate radial vibrations at the double fundamental frequency to both the rotor and the stator [12]. Besides the radial UMP which causes radial vibrations, there is still UMP in the tangential direction and this UMP will significantly affect the stability of the rotor [13]. Researchers have also carried out studies to control UMP by using the damper windings on the rotor in generators [14] and detect SAGE by installing flux probes [15].

In addition to the well-known parameters such as the back EMF, the stator current, the rotor current, the UMP as well as the vibration, etc., people still found that the electromagnetic torque (EMT) is also a good tool to analyze and detect the eccentricity faults [16]. Currently, EMT has been employed to detect the transmission gear fault [17], the field winding interturn short circuit fault [18], and the stator interturn short circuit fault [19]–[22].

Then, what are the comprehensive characteristics of EMT in SAGE cases? Though Z.Q. Zhu *et al.* have found that the EMT harmonics of 8th, 16th, 32nd, and 40th, etc. in

the 8-pole/9-slot PM machine will be increased under SAGE conditions [16], the detailed mapping function between EMT and the influential factors such as the pole-pair numbers, the SAGE degrees, etc., have not been discussed in detail. On one hand, it needs to deduct the detailed EMT formula under SAGE in synchronous generators. On the other hand, it is significant to expand SAGE from 2D to 3D since the air-gap distribution asymmetry can take place not only in the radial direction but also in the axial direction. The axial SAGE, which has a larger axial air-gap length on one end while at the meantime has a smaller axial air-gap length on the other end (between the rotor-core and the housing cover), is potential to take place, especially in hydro-generators due to the long-term water impacts.

By far, scholars have primarily focused on the radial SAGE, especially the parallel/constant SAGE in the radial direction. As an improvement, Dorrell and Salah [2] and Iamamura *et al.* [23] expanded the research from parallel/constant SAGE to non-parallel/non-constant SAGE. That means, the rotor is oblique, i.e., the central line of the rotor forms an angle with the central line of the stator. Actually, the oblique rotor eccentricity will also reduce the action length of the rotor. However, since the oblique angle is very small (the radial air-gap length is small), the equivalent reduction in the axial action length is tiny. Moreover, the axial length of the stator core is usually a little longer than that of the rotor and this length difference can fully compensate the action-length reduction due to the oblique rotor. Therefore, [2] and [23] contributed a great progress, but the SAGE cases they studied still belong to radial SAGE, while the axial SAGE and the hybrid SAGE (eccentricity occurs in both the radial and the axial directions) have not been paid enough attention.

However, the axial SAGE as well as the hybrid SAGE does exist in practice, though the eccentricity degree may not be so large. For example, [24] studied the axial movement (i.e., axial SAGE) and the axial electromagnetic forces of the rotor in hydro-generators, [25] investigated the axial rub-impact fault (which reflects the axial SAGE) in turbo-generator sets, [26] studied the axial movement of a stepper motor. It is actually easy to understand why axial SAGE could be caused in generators: fluid-solid-interaction will produce an axial force on the rotor and after a long-term impact the rotor will get an axial displacement (axial SAGE). For example, the water impact on the rotor system of hydro-generator, the wind action on the rotor system of the wind-turbine generator, and the steam pressure on the blade-rotor system of turbo-generator, may all cause the axial SAGE.

In this paper, we propose a comprehensive study on EMT fluctuation characteristics in radial SAGE, axial SAGE, and hybrid SAGE cases. The remainder of this paper is organized as follows. Section II describes the detailed theoretical model to show the impact of different SAGE types on EMT properties. Section III presents the FEA and experimental results to validate the proposed model. Finally, primary conclusions of this paper are drawn up in Section IV.

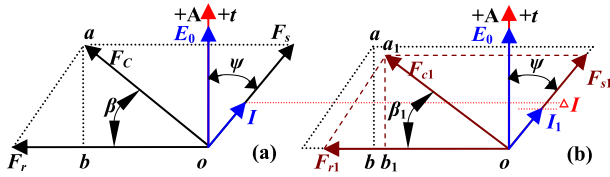


FIGURE 1. Diagram of MMF vectors in (a) normal and radial SAGE cases, and (b) axial SAGE cases.

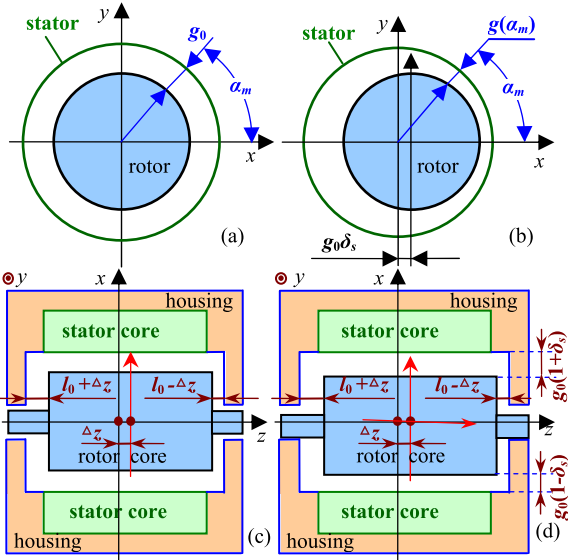


FIGURE 2. Air-gap of generator (a) section view, normal, (b) section view, radial SAGE, (c) front view, axial SAGE, (d) front view, hybrid SAGE.

II. THEORETICAL MODEL

A. IMPACT OF SAGE ON MFD

MFD is composed of MMF and PPUA. In a synchronous generator, the MMF in the air-gap is actually a composite one composed by both the rotor MMF and the stator MMF, as indicated in Fig.1 (a). However, the occurrence of the axial SAGE will actually reduce the effective rotor MMF as well as the stator MMF due to the decrease of the action length, as indicated in Fig.2 (c). And the rotor MMF and the stator MMF in the axial and the hybrid cases are indicated in Fig.1 (b). The final air-gap MMF can be written as

$$f(a_m, t) = \begin{cases} F_s \cos(\omega t - p\alpha_m) + F_r \cos(\omega t - p\alpha_m + \psi + 0.5\pi) \\ \dots \text{normal \& radial SAGE} \\ F_{s1} \cos(\omega t - p\alpha_m) + F_{r1} \cos(\omega t - p\alpha_m + \psi + 0.5\pi) \\ \dots \text{axial \& hybrid SAGE} \end{cases} \quad (1)$$

where $F_{r1} < F_r, F_{s1} < F_s$.

PPUA can be obtained through

$$\Lambda(a_m) = \frac{\mu_0}{g(a_m)} \quad (2)$$

Equation (2) suggests that PPUA should depend on the radial air-gap length which will be affected by radial SAGE,

see Fig.2 (a) and (b). And the radial air-gap length can be written as

$$g(a_m) = \begin{cases} g_0 \dots \dots \dots \text{normal/axial SAGE} \\ g_0(1 - \delta_s \cos \alpha_m) \dots \dots \text{radial/hybrid SAGE} \end{cases} \quad (3)$$

Feed (3) into (2) it finally has

$$\Lambda(a_m) = \begin{cases} \Lambda_0 \dots \dots \dots \\ \dots \dots \dots \text{normal/axial SAGE} \\ \Lambda_0(1 + \delta_s \cos \alpha_m + \delta_s^2 \cos^2 \alpha_m) \\ + \dots \delta_s^3 \cos^3 \alpha_m + \dots \\ \approx \Lambda_0(1 + 0.5\delta_s^2 + \delta_s \cos \alpha_m + 0.5 \cos 2\alpha_m) \\ \dots \dots \dots \\ \dots \dots \dots \text{radial/hybrid SAGE} \end{cases} \quad (4)$$

where the second formula is obtained through the expansion of Power Series.

Then MFD can be further obtained by

$$B(a_m, t) = f(a_m, t) \Lambda(a_m) = \begin{cases} = [F_r \cos(\omega t - p\alpha_m + \psi + 0.5\pi) + F_s \cos(\omega t - p\alpha_m)] \\ \Lambda_0 \dots \dots \dots \text{normal} \\ = [F_r \cos(\omega t - p\alpha_m + \psi + 0.5\pi) + F_s \cos(\omega t - p\alpha_m)] \\ \times \Lambda_0(1 + 0.5\delta_s^2 + \delta_s \cos \alpha_m + 0.5\delta_s^2 \cos 2\alpha_m) \dots \\ \dots \dots \dots \text{radial SAGE} \\ = [F_{r1} \cos(\omega t - p\alpha_m + \psi + 0.5\pi) + F_{s1} \cos(\omega t - p\alpha_m)] \\ \Lambda_0 \dots \dots \dots \text{axial SAGE} \\ = [F_{r1} \cos(\omega t - p\alpha_m + \psi + 0.5\pi) + F_{s1} \cos(\omega t - p\alpha_m)] \\ \times \Lambda_0(1 + 0.5\delta_s^2 + \delta_s \cos \alpha_m + 0.5\delta_s^2 \cos 2\alpha_m) \dots \dots \\ \dots \text{hybrid SAGE} \end{cases} \quad (5)$$

Taking the normal MFD, i.e., the first equation in (5), as the reference, it can be found that the MFD in the radial SAGE case (see the second equation in (5)) will be shifted upward due to the increment of the DC value (in radial SAGE case the DC value is $\Lambda_0 + 0.5\Lambda_0\delta_s^2$, while in normal condition it is only Λ_0). However, in axial SAGE case (see the third equation in (5)), since F_{r1} is smaller than F_r and F_{s1} is smaller than F_s , the MFD will be compressed to a more tabular one. To make the MFD changing tendency more clarified, taking a 2-pole generator as an example, Fig. 3 shows the impact of the radial SAGE and the axial SAGE on MFD. For the hybrid SAGE, it will be influenced by both the radial SAGE and the axial SAGE.

B. EMT BEFORE AND AFTER SAGE

Ignoring the loss, the transformed air-gap magnetic energy should be generally equal to the output electric power as well as the electromagnetic torque energy. The air-gap magnetic energy can be expressed as [18]

$$W = \int_v \frac{[B(a_m, t)]^2}{2\mu_0} dv \quad (6)$$

TABLE 1. EMT component amplitude formulas and influential factors.

condition	DC component (0Hz)	Tendency	2nd harmonic	Tendency
Normal	$pL\Lambda_0R_0\pi F_r F_s \cos\psi$	--	--	--
Radial SAGE	$pL\Lambda_0R_0\pi(1+0.5\delta_s^2)F_r F_s \cos\psi$	↑	$pL\Lambda_0\pi R_0 F_r \delta_s^2 \sqrt{F_r^2 + F_s^2 + 2F_r F_s \sin\psi}$	↑
Axial SAGE	$pL(1-\Delta z)\Lambda_0R_0\pi F_{r1} F_{s1} \cos\psi$	↓	--	--
Hybrid SAGE	$pL(1-\Delta z)\Lambda_0R_0\pi(1+0.5\delta_s^2)F_{r1} F_{s1} \cos\psi$	depends	$pL(1-\Delta z)\Lambda_0\pi R_0 F_{r1} \delta_s^2 \sqrt{F_{r1}^2 + F_{s1}^2 + 2F_{r1} F_{s1} \sin\psi}$	depends
Influential factors	$I_f, p, L, g_0, R_0, \Psi, \delta_s, \Delta z$	--	$I_f, p, L, g_0, R_0, \Psi, \delta_s, \Delta z$	--

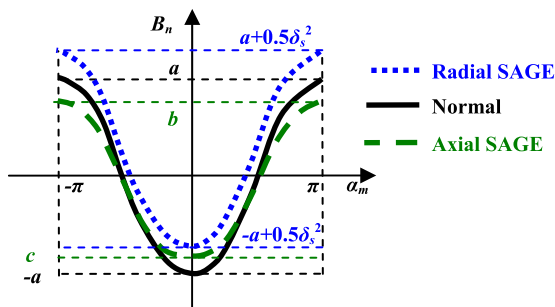


FIGURE 3. Impact of radial SAGE and axial SAGE on MFD.

According to the principle of virtual displacement, as indicated in Fig.1, assuming that $\Delta\psi$ is the differential displacement of the rotor MMF in the spatial position, then the EMT can be obtained by

$$T_e = p \frac{\partial W}{\partial \psi} \tag{7}$$

Based on (6), (7) and Fig.3, to further analyze the EMT variation regularity, we calculate the square of MFD, see Fig.4. For the radial SAGE case, it has the same integral volume as normal condition in (6). However, in axial SAGE cases, the integral volume as well as the MFD square will be decreased due to the reduction of the action length (see Fig.2 c). Therefore, Fig.4 actually reflects the final EMT comparison results. It is distinct that the radial SAGE will increase the EMT amplitude (peak), while the axial SAGE will reduce the EMT amplitude. For the hybrid SAGE cases,

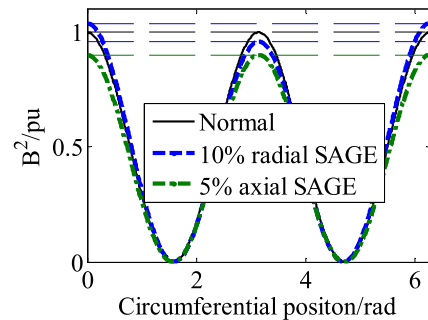


FIGURE 4. Square of MFD.

both the radial SAGE and the axial SAGE will affect EMT, and the final result depends on the detailed degrees of these two SAGE types.

Since the eccentricity in the two directions will act reversed impacts on EMT, it is significant to separate them. Actually, they can be distinguished by the changes in the harmonic composition. Feed (1), (4), and (5), respectively, into (6) and (7), the EMTs before and after SAGE can be finally written in (8), as shown at the bottom of this page. As indicated in (8), for axial SAGE cases, the harmonic components will be the same as the normal condition, only with the harmonic amplitude decreased. However, the occurrence of the radial SAGE will produce extra components at 2ω . To be more clarified, the component amplitude formulas, the developing tendencies, and the influential factors are listed in Tab. 1.

$$T_e = \begin{cases} -pL\Lambda_0R_0\pi F_r F_s \cos\psi \dots\dots\dots \text{normal} \\ -pL\Lambda_0R_0\pi[(1+0.5\delta_s^2)F_r F_s \cos\psi - \delta_s^2 F_r^2 \sin(2\omega t + 2\psi) + \delta_s^2 F_r F_s \cos(2\omega t + \psi)] \dots\dots\dots \text{radial SAGE} \\ -pL(1-\Delta z)\Lambda_0R_0\pi F_{r1} F_{s1} \cos\psi \dots\dots\dots \text{axial SAGE} \\ -pL(1-\Delta z)\Lambda_0R_0\pi[(1+0.5\delta_s^2)F_{r1} F_{s1} \cos\psi - \delta_s^2 F_{r1}^2 \sin(2\omega t + 2\psi) + \delta_s^2 F_{r1} F_{s1} \cos(2\omega t + \psi)] \dots\dots\dots \text{hybrid SAGE} \end{cases} \tag{8}$$

TABLE 2. Parameters of CS-5 prototype generator.

Parameters	Value	Parameters	Value
Rated Capacity	5kVA	Rated voltage	380V
Rated rotating speed	$n_r=3000\text{rpm}$	Pole pairs	$p=1$
Power factor	$\cos\varphi=0.8$	Stator slots	$Z_1=36$
Radial air-gap length	1.2 mm	Pitch distance	14
Stator core length	$l=130\text{ mm}$	Exciting turns	480
Turns per phase	264	Parallel branches	$a=2$

Actually, (8) is the EMT result which only considers the fundamental-frequency MMFs (see Fig.1). Since the exciting current is DC, the *Fourier Series* of rotor MMF include only odd harmonics. Consequently, the stator MMF also includes only odd harmonics. Taking the higher order harmonics into account, there should be even harmonics in both normal conitron and SAGE cases, detailed analysis process about this can be found in [27].

III. FEA AND EXPERIMENT VALIDATION

A. FEA AND EXPERIMENT SETUP

The finite element analysis and the experiment study are carried out on the CS-5 prototype generator in State Key Laboratory of Alternate Electrical System with Renewable Energy Sources, P.R. China, as shown in Fig.5 and Table 2.

The rotor is kept stable to the foundation by the bearing blocks, while the stator can be moved along the horizontally radial direction by two adjustment screws on the front side (along X axis, see Fig.5 a) and another two screws on the back side (reversed to X axis, see Fig.5 a). At the meantime, the stator can be also moved along the horizontally axial direction by two adjustment screws on the driven end (right side in Fig.5 b, along Z axis in Fig.5 a) and another two screws on the non-driven end (left side in Fig.5 b, reversed to Z axis in Fig.5 a). The movements in these two directions can be controlled by four dial indicators, two for the radial direction and another two for the axial direction.

During experiment and FEA, the exciting current was set to 2.5A, and the load for each phase is a 100 Ohm resistance and a 0.238 H inductance ($\cos\varphi = 0.8$), as indicated in Fig.5 (e). In the experiment EMT is obtained through

$$T_e(t) = \frac{P(t)}{\omega(t)} = \frac{[U_a(t)I_a(t) + U_b(t)I_b(t) + U_c(t)I_c(t)] \cos \varphi}{2\pi n/60} \tag{9}$$

Experiments and FEA calculation are taken for 13 times respectively for:

- 1) normal condition.
- 2) 0.1-mm, 0.2-mm, and 0.3-mm RSAGE cases.
- 3) 3-mm, 6-mm, and 9-mm ASAGE cases.
- 4) HSAGE cases with 6-mm ASAGE and 0.1-mm, 0.2-mm, and 0.3-mm RSAGE, respectively.
- 5) HSAGE cases with 0.2-mm RSAGE and 3-mm, 6-mm, and 9-mm ASAGE, respectively.

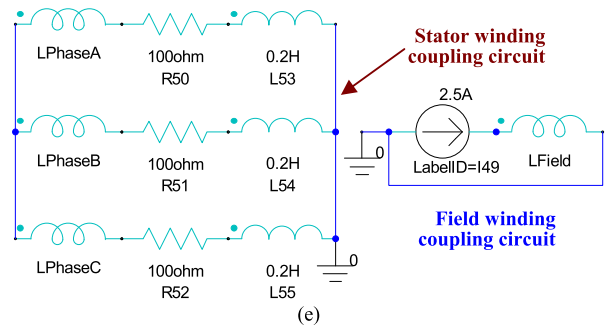
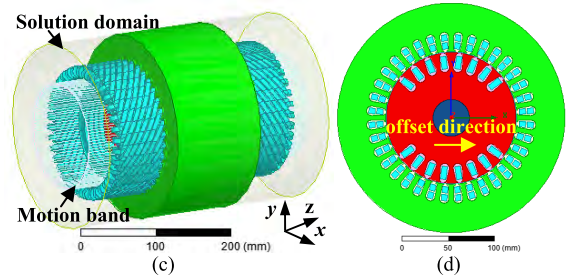
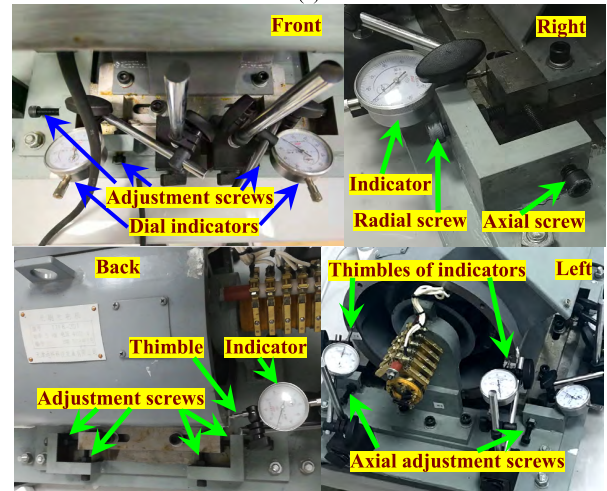
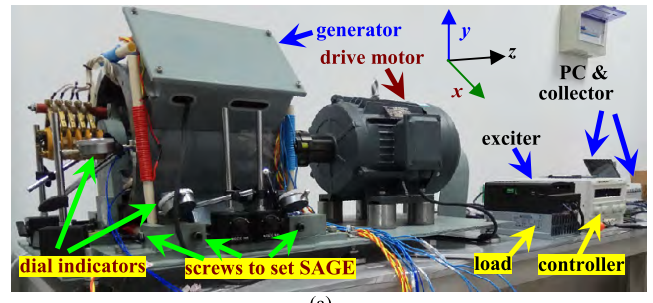


FIGURE 5. CS-5 prototype generator (a) general outlook picture, (b) method to set radial and axial SAGE, (c)FE model, (d) section view of model with radial SAGE, (e) external coupling circuit model.

Specifically, during FEA we employ a full 3D model to obtain a more comprehensive and accurate result. Actually, 2D FEA model is only qualified for radial SAGE, while it does not meet the requirement of axial SAGE and hybrid SAGE. Primary concern about this lies in two issues: 1) 2D FEA which simulates axial eccentricity by changing

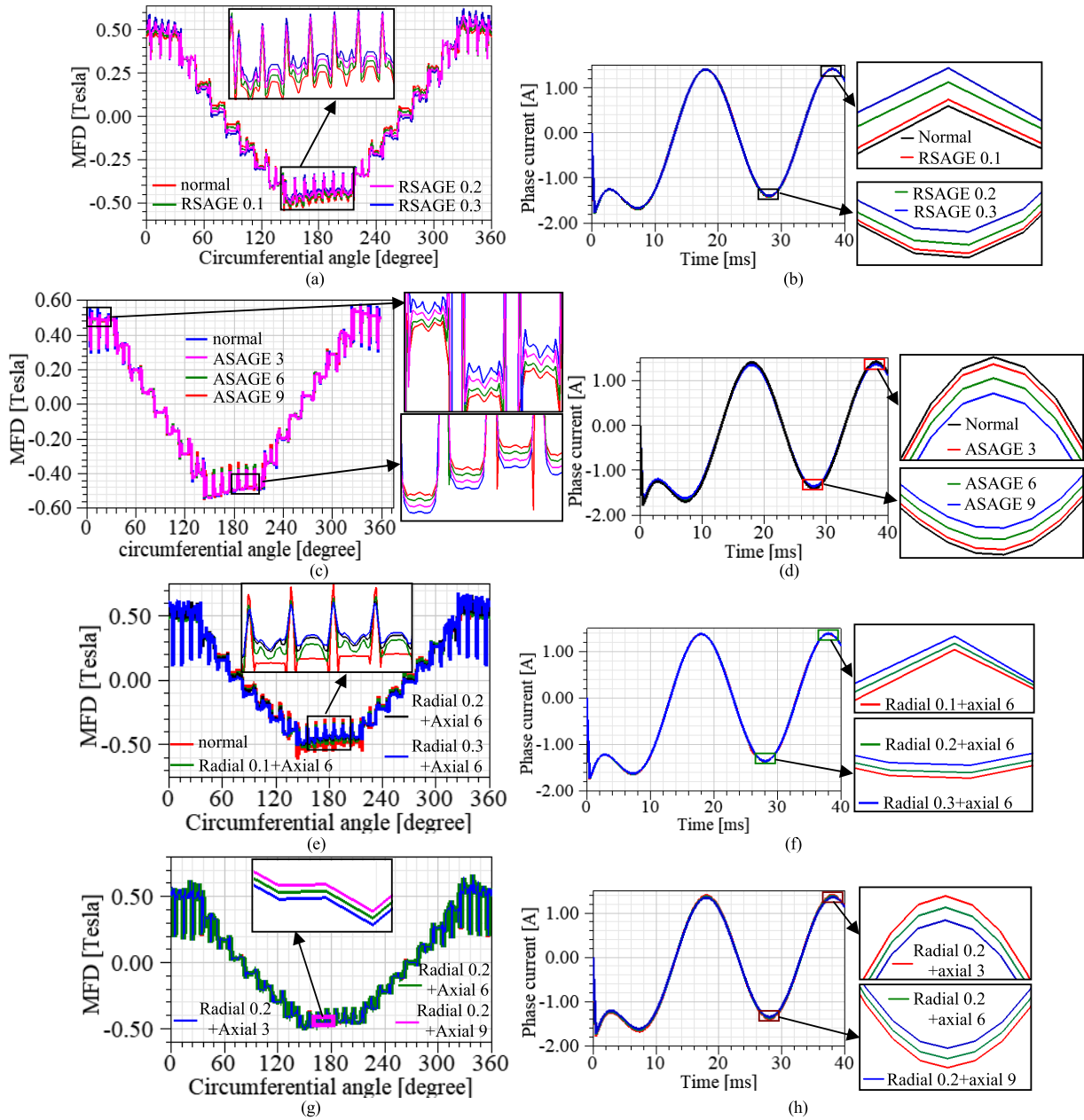


FIGURE 6. MFD and phase current obtained by FEA: (a)-(b) MFD and phase current in RSAGE cases, (c)-(d) MFD and phase current in ASAGE cases, (e)-(f) MFD and phase current in HSAGE cases with RSAGE increased, (g)-(h) MFD and phase current in HSAGE cases with ASAGE increased.

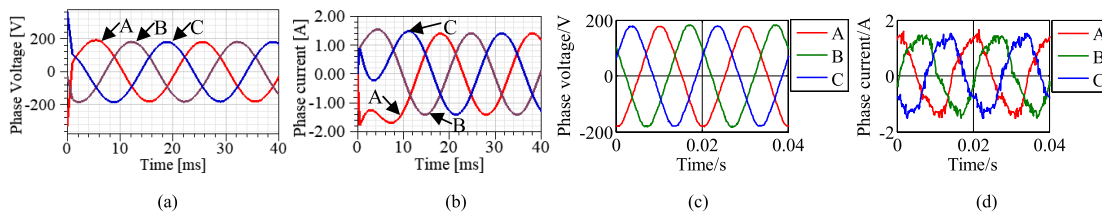


FIGURE 7. Normal Phase voltage and current (a) and (b) FEA results, and (c) and (d) experimental results.

the action length of stator/rotor will adjust the axial air-gap length on both the two ends at the same time with the same extent, i.e., the axial air-gap lengths on the two ends

are still equal. However, the eccentricity requires the air-gap to be larger on one end while smaller on the other end. 2) 2D FEA is not able to take the flux leakage on the end

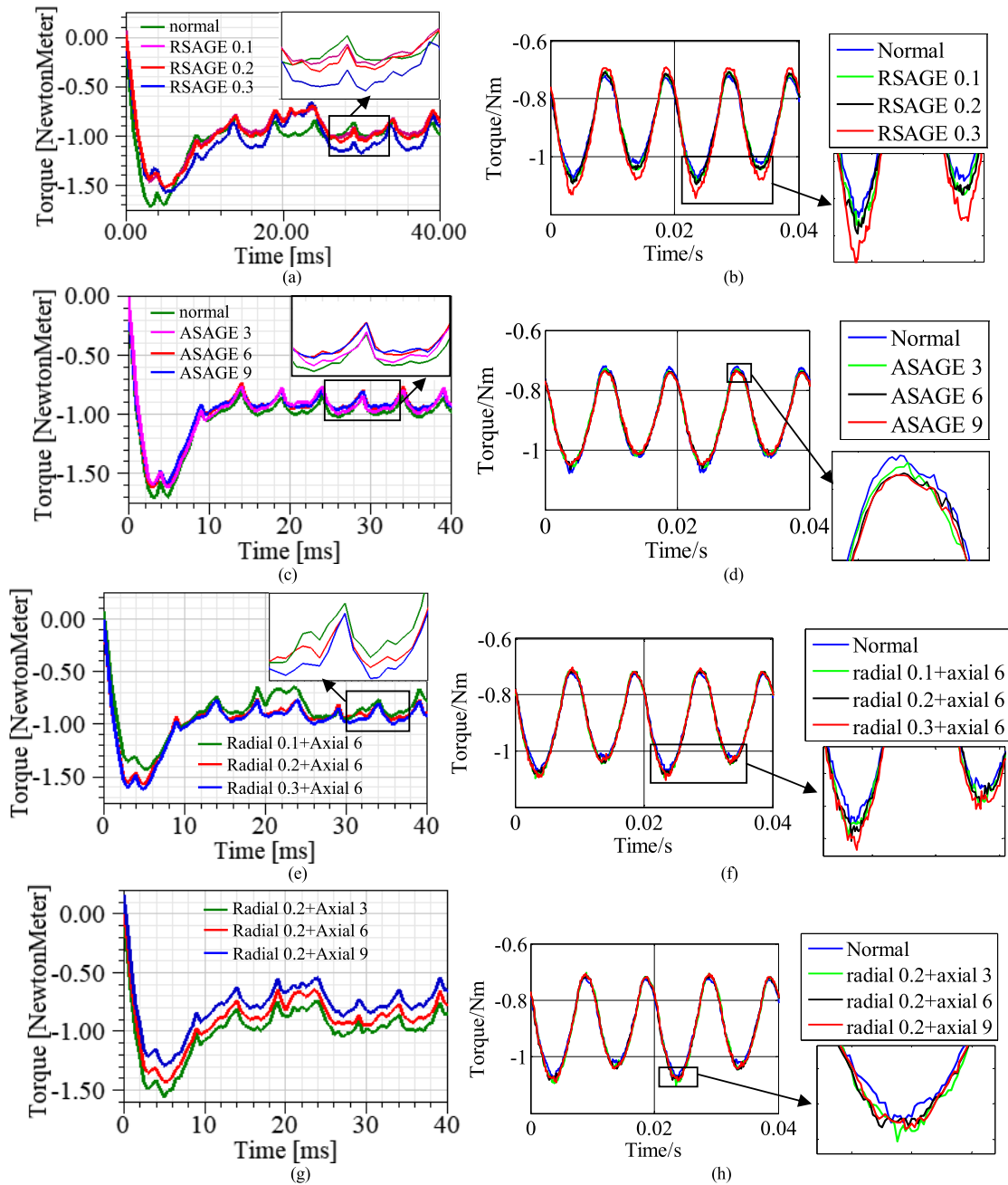


FIGURE 8. EMT waveforms obtained by FEA (left) and experiment (right): (a)-(b) RSAGE cases, (c)-(d) ASAGE cases, (e)-(f) HSAGE cases with RSAGE increased, and (g)-(h) HSAGE cases with ASAGE increased.

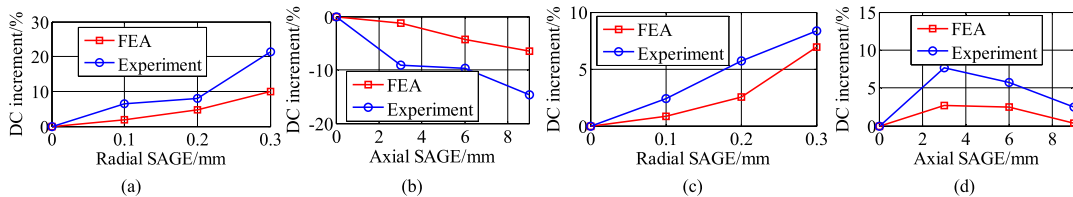


FIGURE 9. DC EMT increment (a) RSAGE, (b) ASAGE, (c) HSAGE with RSAGE increased, and (d) HSAGE with ASAGE increased.

side into account. Since the air-gap on the two ends is not equal, the impact of the flux leakage on MFD will also be different.

B. RESULTS AND DISCUSSION

The air-gap MFD at 0.02s and the phase current in different SAGE cases obtained from FEA are indicated in Fig.6.

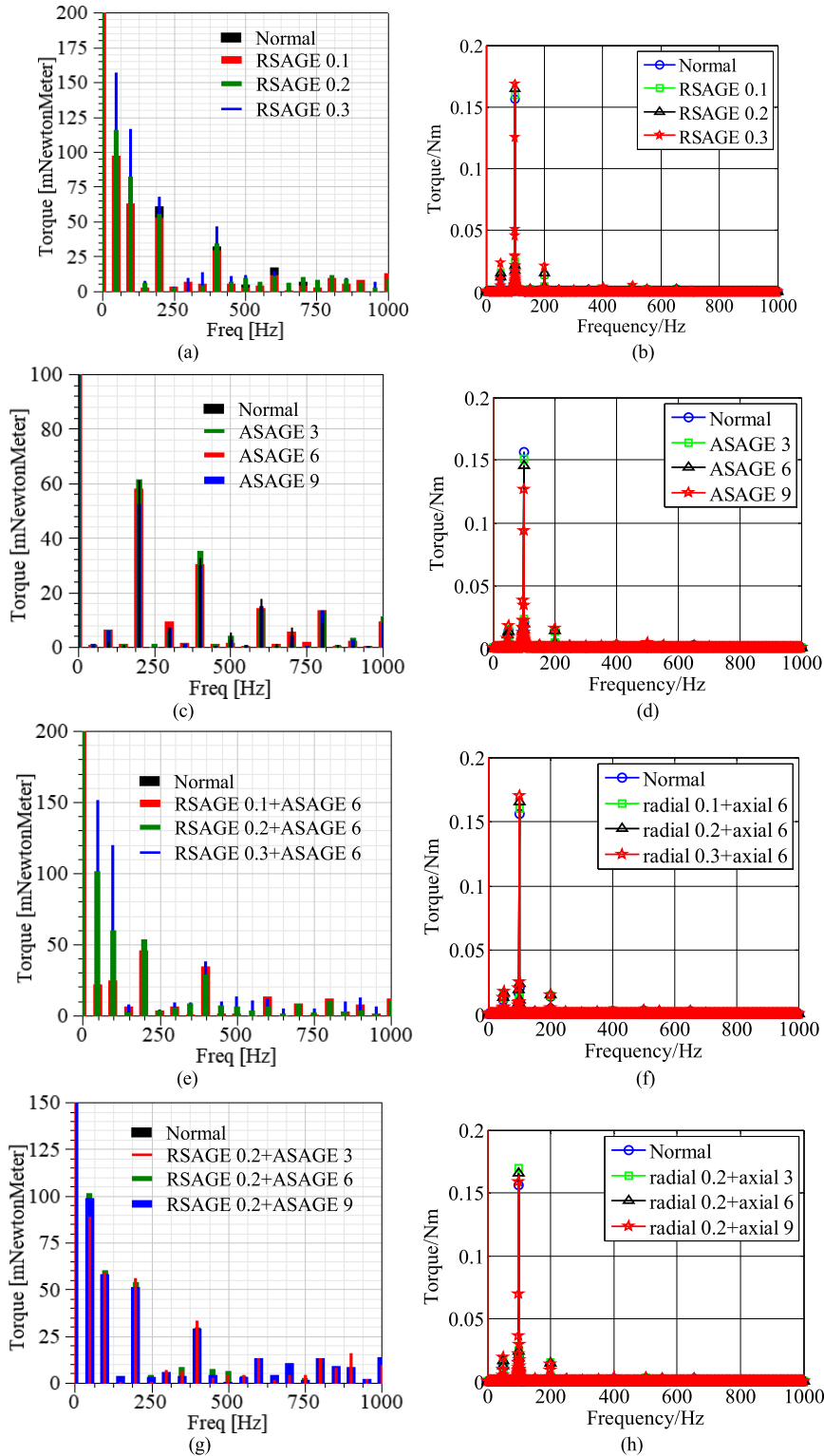


FIGURE 10. EMT Spectra by FEA (left) and experiment (right): (a)-(b) RSAGE cases, (c)-(d) ASAGE cases, (e)-(f) HSAGE cases with RSAGE increased, (g)-(h) HSAGE cases with ASAGE increased.

The radial eccentricity direction is along the X-axis (to the right, see Fig.5 d), the axial eccentricity is along the Z-axis (to the driven end, see Fig.5 a), and the probe air-gap section is in the middle of the stator core length.

As indicated in Fig. 6, both MFD and the phase current in RSAGE cases will be shifted upward (just like an upward movement), while in ASAGE cases MFD and the phase current will be reduced (just like a compressing operation).

In HSAGE cases, the increment of RSAGE will still shift the MFD and the phase current upwardly, while the increment of ASAGE will still reduce MFD and the phase current. The results shown in Fig.6 are quite consistent to the theoretical analysis (see Fig.3). Since the phase current is a significant reflect of MFD, the accordance of the MFD and the phase current suggests the validation of the previous theoretical analysis (it is hard to test the MFD during the rotor is rotating due to the very small air-gap length).

The phase voltage and phase current in normal condition are indicated in Fig.7. Limited by space, voltage and current comparisons between FEA and experiments for other cases are not listed here. It is suggested from Fig.7 that the tested phase voltages and currents generally match well with the FEM-calculated ones.

The EMT waveforms obtained from finite element calculation and experiments are illustrated in Fig.8. Generally, the FEA data shows a more obvious tendency while the tested curves are much more complex (the curves are not so uniformed and they intertwine with each other) due to many practical influential factors. However, the experimental result still follows the developing trend obtained from the finite element calculation. It is shown that for both unidirectional and hybrid SAGE conditions, RSAGE will generally increase the EMT fluctuation amplitude, while ASAGE will reduce the EMT amplitude. Also, Fig.8 is in accordance with Fig.4, which suggests that the FEA and the experimental results coincide with the previous theoretical result.

During the actual monitoring, besides the EMT waveforms, the specific component variation (the spectrum change) will be helpful to identify the exact SAGE types. The amplitude variation of the DC components is indicated in Fig.9, while changes of other harmonic components are displayed in Fig.10.

As indicated in Fig.9, in both unidirectional and hybrid SAGE cases, RSAGE will primarily increase the DC amplitude, while ASAGE will decrease the DC value. This result is in good accordance with (5).

EMT spectrum changes indicated in Fig.10 suggest that RSAGE will generally increase the amplitude of each harmonic, especially at 50 Hz, 100 Hz, and 200 Hz (the basic frequency is 50Hz). However, ASAGE will act an inversed impact on the harmonic amplitudes. Comparatively, even harmonics have a more obvious variation than the odd ones. This phenomenon follows the qualitatively theoretical analysis in Section II (see (8) and Tab. 1).

In addition, it is also studied in [9] that SAGE will affect the phase voltage (phase current). The 3rd harmonic as well as 9th, 15th, etc., will be increased. More details can be found in Figs. 11 and 12 in [9] and will not be repeated here. The difference between the phase current signature and EMT is that EMT may even enlarge the harmonic difference between healthy and faulty conditions, since EMT is in proportion to the current square (see Equation 9, where the numerator equals to $3I^2R\cos\varphi$, i.e., the output power). Thus, EMT can be a good tool/ supplement.

Practically, the axial eccentricity may be not stable during the machine is running because of many impact factors. For example, the rotor may display its axial eccentricity in the form of always changing from 4mm to 6mm. However, either the dynamic eccentricity or the stable eccentricity should have a degree (for example, 0mm-2mm is a slight degree while 4mm-6mm is a severer degree). Consequently, EMT will appear variations as well due to the degree difference. And this variation regularity is generally similar to the static cases. In fact, the dynamic eccentricity condition can be treated as the combinations of many different static eccentricity cases. Limited by space, we will carry out another work in the short future to specifically study the dynamic eccentricity.

IV. CONCLUSION

This paper presents a comprehensive study on the impact of 3D SAGE on EMT ripple properties. Detailed EMT expressions as well as the MFD formulas in normal condition and different SAGE cases are obtained by theoretical deduction. These expressions can be used for the fast EMT assessment and the harmonic amplitude developing tendency prediction, while the MFD formulas can be further employed as the basis of other MFD-related parameter studies such as the rotor unbalanced magnetic pull which is in proportion to the square of MFD.

3D finite element calculation and experimental study on a CS-5 prototype generator which is of two poles and 3000 rpm are carried out for the validation of the theoretical analysis. The FEA data and the experimental result well follow the qualitative analysis presented in the theoretical model section. It is shown that the radial SAGE will increase the DC component of MFD and shift the whole MFD curve and the phase current upwardly, while the axial SAGE will reduce the DC component and the amplitudes of both the MFD and the phase current like a compressing operation. Generally, no matter in unidirectional or hybrid SAGE cases, the radial SAGE will intensify the EMT ripple and increase each harmonic of EMT, while axial SAGE will play the opposite role. These useful conclusions are potential to be applied as a supplement criterion for the condition monitoring and control of SAGE faults.

REFERENCES

- [1] M.-F. Hsieh and Y.-H. Yeh, "Rotor eccentricity effect on cogging torque of PM generators for small wind turbines," *IEEE Trans. Magn.*, vol. 49, no. 5, pp. 1897–1900, May 2013.
- [2] D. G. Dorrell and A. Salah, "Detection of rotor eccentricity in wound rotor induction machines using pole-specific search coils," *IEEE Trans. Magn.*, vol. 51, no. 11, Nov. 2015, Art. no. 8111604.
- [3] D.-J. Kim, H.-J. Kim, J.-P. Hong, and C.-J. Park, "Estimation of acoustic noise and vibration in an induction machine considering rotor eccentricity," *IEEE Trans. Magn.*, vol. 50, no. 2, pp. 857–860, Feb. 2014.
- [4] Z. Nasiri-Gheidari and F. Tootoonchian, "Axial flux resolver design techniques for minimizing position error due to static eccentricities," *IEEE Sensors J.*, vol. 15, no. 7, pp. 4027–4034, Jul. 2015.
- [5] J.-Y. Lee, D.-K. Hong, B.-C. Woo, D.-S. Joo, Y.-H. Chio, and B.-U. Nam, "Unbalanced magnetic force calculation for assembly jig design," *IEEE Trans. Magn.*, vol. 48, no. 11, pp. 4224–4227, Nov. 2012.
- [6] Y.-L. He, W.-Q. Deng, G.-J. Tang, X.-L. Sheng, and S.-T. Wan, "Impact of different static air-gap eccentricity forms on rotor UMP of turbogenerator," *Math. Problems Eng.*, vol. 2016, Jun. 2016, Art. no. 5284815.

- [7] J. J. Pérez-Loya, C. J. D. Abrahamsson, and U. Lundin, "Electromagnetic losses in synchronous machines during active compensation of unbalanced magnetic pull," *IEEE Trans. Ind. Electron.*, vol. 66, no. 1, pp. 124–131, Jan. 2019.
- [8] L. T. Rosenberg, "Eccentricity, vibration, and shaft currents in turbine generators," *Trans. Amer. Inst. Elect. Eng. III, Power App. Syst.*, vol. 74, no. 3, pp. 38–41, Jan. 1955.
- [9] C. Bruzzese and G. Joksimovic, "Harmonic signatures of static eccentricities in the stator voltages and in the rotor current of no-load salient-pole synchronous generators," *IEEE Trans. Ind. Electron.*, vol. 58, no. 5, pp. 1606–1624, May 2011.
- [10] C. Bruzzese, "Diagnosis of eccentric rotor in synchronous machines by analysis of split-phase currents—Part I: Theoretical analysis," *IEEE Trans. Ind. Electron.*, vol. 61, no. 8, pp. 4193–4205, Aug. 2014.
- [11] C. Bruzzese, "Diagnosis of eccentric rotor in synchronous machines by analysis of split-phase currents—Part II: Experimental analysis," *IEEE Trans. Ind. Electron.*, vol. 61, no. 8, pp. 4206–4216, Aug. 2014.
- [12] S. Wan and Y. He, "Investigation on stator and rotor vibration characteristics of turbo-generator under air gap eccentricity fault," *Trans. Can. Soc. Mech. Eng.*, vol. 35, no. 2, pp. 161–176, Mar. 2011.
- [13] Y. Calleecharan and J.-O. Aidanpää, "Stability analysis of an hydropower generator subjected to unbalanced magnetic pull," *IET Sci., Meas. Technol.*, vol. 5, no. 6, pp. 231–243, Nov. 2011.
- [14] M. Wallin, J. Bladh, and U. Lundin, "Damper winding influence on unbalanced magnetic pull in salient pole generators with rotor eccentricity," *IEEE Trans. Magn.*, vol. 49, no. 9, pp. 5158–5165, Sep. 2013.
- [15] W. Doorsamy, A. A.-E. Abdalh, W. A. Cronje, and L. Dupré, "An experimental design for static eccentricity detection in synchronous machines using a Cramér–Rao lower bound technique," *IEEE Trans. Energy Convers.*, vol. 30, no. 1, pp. 254–261, Mar. 2015.
- [16] Z. Q. Zhu, L. J. Wu, and M. L. M. Jamil, "Distortion of back-EMF and torque of PM brushless machines due to eccentricity," *IEEE Trans. Magn.*, vol. 49, no. 8, pp. 4927–4936, Aug. 2013.
- [17] M. H. Marzabali, J. Faiz, G.-A. Capolino, S. H. Kia, and H. Henao, "Planetary gear fault detection based on mechanical torque and stator current signatures of a wound rotor induction generator," *IEEE Trans. Energy Convers.*, vol. 33, no. 3, pp. 1072–1085, Sep. 2018.
- [18] L. Hao, J. Wu, and Y. Zhou, "Theoretical analysis and calculation model of the electromagnetic torque of nonsalient-pole synchronous machines with interturn short circuit in field windings," *IEEE Trans. Energy Convers.*, vol. 30, no. 1, pp. 110–121, Mar. 2015.
- [19] Y. Liu, R. Qu, J. Wang, H. Fang, X. Zhang, and H. Chen, "Influences of generator parameters on fault current and torque in a large-scale superconducting wind generator," *IEEE Trans. Appl. Supercond.*, vol. 25, no. 6, Dec. 2015, Art. no. 5204309.
- [20] S. E. Dallas, A. N. Safacas, and J. C. Kappatou, "Interturn stator faults analysis of a 200-MVA hydrogenerator during transient operation using FEM," *IEEE Trans. Energy Convers.*, vol. 26, no. 4, pp. 1151–1160, Dec. 2011.
- [21] L. Trilla, J. Pegueroles, J. Urresty, C. Muñoz, and O. Gomis-Bellmunt, "Generator short-circuit torque compensation in multichannel wind turbines," *IEEE Trans. Ind. Electron.*, vol. 64, no. 11, pp. 8790–8798, Nov. 2017.
- [22] Y.-L. He, F.-L. Wang, G.-J. Tang, and M.-Q. Ke, "Analysis on steady-state electromagnetic characteristics and online monitoring method of stator inter-turn short circuit of turbo-generator," *Electr. Power Compon. Syst.*, vol. 45, no. 2, pp. 198–210, 2017.
- [23] B. A. T. Iamamura, Y. Le Menach, A. Tounzi, N. Sadowski, and E. Guillot, "Study of static and dynamic eccentricities of a synchronous generator using 3-D FEM," *IEEE Trans. Magn.*, vol. 46, no. 8, pp. 3516–3519, Aug. 2010.
- [24] J. Qiu and W. Duan, "Axial displacement and axial electromagnetic force of rotor system in hydroturbine generator," *J. Mech. Strength*, vol. 25, no. 3, pp. 285–289, Mar. 2003.
- [25] Z.-W. Yuan, Z.-N. Li, S.-B. Wang, X.-M. Yue, and F.-L. Chu, "Dynamic analysis in full degrees of freedom of rotor's axial rub-impact with consideration of nonlinear fluid-structure interaction forces," *Proc. Chin. Soc. Elect. Eng.*, vol. 28, no. 14, pp. 92–97, May 2008.
- [26] J. Škofic and M. Boltežar, "Numerical modelling of the rotor movement in a permanent-magnet stepper motor," *IET Electr. Power Appl.*, vol. 8, no. 4, pp. 155–163, Apr. 2014.
- [27] J.-Q. Wang, P.-C. Song, C.-H. Cui, J.-K. Li, and T. Yang, "Analysis of operation of synchronous generator under the distortion of harmonic current," in *Proc. Asia-Pacific Power Energy Eng. Conf.*, Shanghai, China, Mar. 2012, pp. 1–4.
- [28] K. Grzybacz, K. Łatak, and T. J. Sobczyk, "Spectral current analysis for high power turbo-generators at internal asymmetry of windings," in *Proc. IEEE 11th Int. Symp. Diagnostics Elect. Mach., Power Electron. Drives (SDEMPED)*, Tinos, Greece, Aug./Sep. 2017, pp. 441–447.



YU-LING HE was born in Fujian, China, in 1984. He received the B.S. degree in mechanical engineering, the B.S. degree in electrical engineering, the M.S. degree in mechatronics engineering based on early graduation due to academic excellence, and the Ph.D. degree in power machinery and engineering from North China Electric Power University, Baoding, China, in 2007, 2009, and 2012, respectively.

From 2012 to 2015, he was an Assistant Professor with the Department of Mechanical Engineering, North China Electric Power University, where he is currently an Associate Professor and the Head of the Mechatronics Engineering. His research interests include condition monitoring and control on electric machines, signal analysis and processing, testing technology, and mathematical modeling in engineering.

Dr. He was awarded as an excellent graduate of Beijing City from North China Electric Power University. He is an Editorial Member of three international journals, the Hebei Provincial Top Youth Talent, the 3-3-3 Project Talent of Hebei Province, and also the Secretary General of Hebei Provincial Society for Vibration Engineering.



MING-XING XU was born in Jiangxi, China, in 1994. He received the B.S. degree in mechanical engineering from North China Electric Power University, in 2017, China, where he is currently pursuing the M.S. degree in mechatronics engineering.

His research interests include faulty characteristic analysis and monitoring on large synchronous generators.



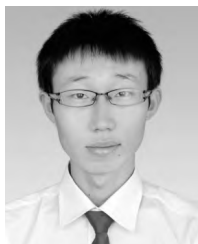
JING XIONG was born in Fujian, China, in 1998. He is currently pursuing the bachelor's degree in electrical engineering with North China Electric Power University, Baoding, China.

His research interest includes electric machine design and improvement.



YUE-XIN SUN was born in Hebei, China, in 1994. She received the B.S. degree in mechanical engineering from North China Electric Power University, China, in 2017, where she is currently pursuing the M.S. degree in mechatronics engineering.

Her research interests include condition monitoring and fault diagnosis on large synchronous generators.



XIAO-LONG WANG was born in Heilongjiang, China, in 1989. He received the B.S. degree in mechanical engineering and the Ph.D. degree in power machinery and engineering from North China Electric Power University, Baoding, China, in 2012 and 2017, respectively.

He is currently an Assistant Professor with the Department of Mechanical Engineering, North China Electric Power University. His research interests include intelligent fault identification, signal analysis and processing, and testing technology.



DAVID GERADA received the Ph.D. degree in high-speed electrical machines from the University of Nottingham, Nottingham, U.K., in 2012.

From 2007 to 2016, he was with the R&D Department, Cummins Inc., where he pioneered the design and development of high-speed electrical machines, transforming a challenging technology into a reliable one suitable for the transportation market and establishing industry-wide used metrics for such machinery. In 2016,

he joined the University of Nottingham as a Senior Fellow in electrical machines, responsible for developing the state-of-the-art electrical machines for future transportation which push existing technology boundaries while propelling the new technologies to high technology readiness levels (TRL). He is currently a Chartered Engineer in U.K. His research interests include novel materials and applications in electromechanical energy conversion, traction machines, and mechatronics.

Dr. Gerada is a member of the Institution of Engineering and Technology.



GAURANG VAKIL (M'16) received the Ph.D. degree in variable-speed generator design for renewable energy applications from the Power Electronics, Machines, and Drives Group, Indian Institute of Technology Delhi, New Delhi, India, in 2016.

After graduation, he subsequently worked as a Research Associate with the Power Electronics, Machines, and Control Group, University of Nottingham, Nottingham, U.K., where he became an

Assistant Professor with the Department of Electrical and Electronics Engineering, in 2016. His main research interests include analytical modeling and design optimization of electrical machines, optimizing electric drive train for pure electric and hybrid vehicles, high-power-density machines, magnetic material characterization, and high-performance electrical machines for transport and renewable generation.

• • •